

*Article*

# X-Band Front-end Module of FMCW RADAR for Collision Avoidance Application

Tiwat Pongthavornkamol<sup>1,a,\*</sup>, Aman Worasutr<sup>2,b</sup>, Denchai Worasawate<sup>2,c</sup>,  
La-or Kovavisaruch<sup>1,d</sup>, and Kamol Kaemarungsi<sup>1,e</sup>

<sup>1</sup> Location and Automatic Identification System Research Team, Communications and Networks Research Group, National Electronics and Computer Technology Center (NECTEC), 112 Thailand Science Park, Phahonyothin Road, Khlong Nueng, Khlong Luang, Pathum Thani 12120, Thailand

<sup>2</sup> Department of Electrical Engineering, Faculty of Engineering, Kasetsart University, 50 Ngamwongwan Road, Ladyao, Chatuchak, Bangkok 10900, Thailand

E-mail: <sup>a,\*</sup>[tiwat.pon@nectec.or.th](mailto:tiwat.pon@nectec.or.th) (Corresponding author), <sup>b</sup>[man\\_d\\_wora@hotmail.com](mailto:man_d_wora@hotmail.com),  
<sup>c</sup>[fengdcw@ku.ac.th](mailto:fengdcw@ku.ac.th), <sup>d</sup>[la-or.kovavisaruch@nectec.or.th](mailto:la-or.kovavisaruch@nectec.or.th), <sup>e</sup>[kamol.kaemarungsi@nectec.or.th](mailto:kamol.kaemarungsi@nectec.or.th)

**Abstract.** A frequency modulated continuous wave (FMCW) radar front-end module is developed as a laboratory prototype of NECTEC, NSTDA. The performance of proposed prototype is verified by the reflection test of aluminum plates in outdoor environment. The frequency domain data from a spectrum analyzer was measured at every 20 meters of the distance between the front-end prototype and the aluminum plate until the maximum distance of 200 meters is reached. The calculation of the beat frequencies at different range of reflecting aluminum plates is presented. The maximum error between measured and calculated distances does not exceed 5.02 percent. The effect of different radar cross section (RCS) of reflecting objects of 0.3, 0.8 and 1.5 m<sup>2</sup> plate area are analyzed. The low value of different received power ratio per one squared meter unit area of 0.66 percent is obtained to prove the consistency of reflected power level over the different size of object under test.

**Keywords:** RADAR, FMCW, beat frequency, RCS.

**ENGINEERING JOURNAL** Volume 25 Issue 5

Received 5 October 2020

Accepted 12 April 2021

Published 31 May 2021

Online at <https://engj.org/>

DOI:10.4186/ej.2021.25.5.61

## 1. Introduction

In Thailand, the automobile for the future, the digital industry, and the aviation & logistics are considered as s-curve industries in the vision of fourth industrial revolution [1]. One of the key technologies that can play an important role in these industries is the Radio Detection and Ranging (RADAR) sensor technology which is important for surveying, searching, detecting, and tracking applications. For instance, RADAR technologies are applied in applications such as through wall RADAR (Ultra Wideband 3-10 GHz) [2], indoor localization RADAR [3], Earth imaging RADAR via satellite [4] and collision avoidance RADAR for automotive vehicle (W-Band 76-81 GHz [5-6] or K-Band 18-25 GHz [7]). Due to the high cost of these high frequency RADAR prototypes, the frequency modulated continuous wave (FMCW) RADAR operated in lower frequency band (X-Band 8-12 GHz) can be an alternative for collision avoidance system in ground transportation. In this work, we investigated on the calculated beat frequencies at different ranges of reflecting object. The beat frequency is the difference value between transmitted frequency and received frequency that is used to attain the range and velocity information [8-9]. The results showed that the calculated beat frequencies have slightly difference from simulated values. The maximum detectable range of 200 meters is achieved from the outdoor field test.

## 2. FMCW RADAR System

Frequency modulated continuous wave (FMCW) radar is a well-established technique published by Strauch in 1976 [10-11]. The technique was initially used for operating FMCW radars at low transmitting frequencies. There are many advantages of FMCW RADAR over the pulsed RADAR in terms of higher range accuracy and safety from the absence of pulse radiation with high peak power. In FMCW RADAR system, a transmitted signal is processed by frequency modulation to continuously increase the transmitted signal frequency until the frequency reach the highest level. Then the signal frequency drops to the starting frequency for the next iteration of frequency increment. At the same time, the analysis of received signal's frequency is performed in each iteration.

In this technique, a signal is transmitted while the transmitter increases its frequency periodically. When an echo signal is received, the receiver determines the change of frequency as it gets a delay ( $\Delta t$ ) like the technique of pulse RADAR. The representation of frequency modulation is shown in Fig. 1 where the red line represents the transmitted signal and green line represents received signal. When the reflecting object is approaching or departing the RADAR system, the doppler frequency ( $f_d$ ) occurs as positive or negative value, respectively.

If the increment of the transmitted frequency is linearly related with the time, the range between RADAR and the reflecting object can be calculated by Eq. (1). The

measured frequency difference ( $\Delta f$ ) is also proportional to the range value.

$$R = \frac{c_0 \cdot |\Delta t|}{2} = \frac{c_0 \cdot |\Delta f|}{2 \cdot \frac{df}{dt}} \quad (1)$$

where

$c_0$  = Velocity of light in free space ( $3 \times 10^8$  m/sec)

$\Delta t$  = Time delay

$\Delta f$  = Measured frequency difference

$R$  = Distance between antenna and reflecting object

$df/dt$  = Frequency shift per unit of time

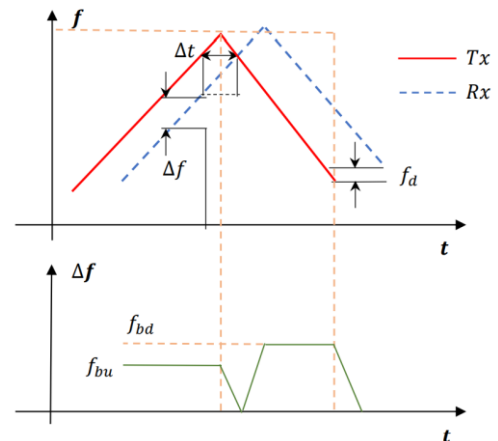


Fig. 1. Transmitted Signal (red solid line) and Received Signal (blue dash line) with frequency sweeping [11].

The different value between transmitted and received signals can be called as beat frequency ( $f_b$ ). The beat frequency is an important parameter to calculate the distance between RADAR and the reflecting object. The FMCW RADAR range equation is shown in Eq. (2).

$$R = \frac{c T_s f_b}{2B} \quad (2)$$

where

$c$  = Velocity of Light in Free Space ( $3 \times 10^8$  m/sec)

$T_s$  = Period of Sawtooth signal for controlling RF Signal Synthesizer (sec)

$B$  = Bandwidth of RF Signal Synthesizer (Hz)

$f_b$  = Difference between transmitted and received signals or Beat frequency (Hz)

## 3. FMCW X-Band Front-end Module

This section provides details of FMCW X-Band frontend module that can be implemented as a subsystem of FMCW RADAR system. The X-Band frequencies are good candidate for the detection of normal size object such as cars, motorcycles, humans and UAVs. The frontend module was developed from common off the shelf development boards. The specification and capabilities of the system are summarized in Table 1. The operating frequencies of 9.4-9.7 GHz are selected by the

limitation of X-Band synthesizer as it can only response to the 4 V to 9 V frequency modulated waveform with maximum chirp sampling frequency of 267 Hz. The minimum received power of -100 dBm is estimated from the detectable capability of the handheld spectrum analyzer.

Table 1. Specification of X-Band FMCW RADAR Frontend Module.

Parameters	Description/Value
RADAR Type	FMCW
Frequency Range	9.4-9.7 GHz
P <sub>out</sub> of Frontend	0.25 W
Tx Antenna Gain	100 (20 dBi)
Rx Antenna Gain	39.81 (16 dBi)
Minimum P <sub>r</sub>	-100 dBm

### 3.1. Radar Range and Power Equations

In order to estimate the required sensitivity of the receiver of the system setup, some parameters such as operating frequencies, output power, antennas gain and RADAR cross section (RCS) are analyzed by using RADAR maximum range given by Eq. (3) and maximum RCS of a flat conducting plate with the width of  $w$  and the height of  $h$  given by Eq. (4), respectively [12].

$$R_{max} = \sqrt[4]{\frac{P_t G_t G_r \lambda^2 \sigma_{max}}{(4\pi)^3 P_{rmin}}} \quad (3)$$

$$\sigma_{max} = \frac{4\pi w^2 h^2}{\lambda^2} \quad (4)$$

By substitution of parameter values from Table 1. into Eq. (3) and (4), the calculated maximum range of the detection is approximately 3450 meters. The calculated maximum RCS of 1.5×1.0 m<sup>2</sup> aluminum plate by equation (4) is approximately 27759 m<sup>2</sup> from assumed values of P<sub>rmin</sub> of -100 dBm and 9.4 GHz of frequency.

The different ranges of object under test from the radar system and the calculated received power required for the radar system detection are listed in Table 1.1. The minimum received power can be calculated by substituting R<sub>max</sub> with the different ranges (R) of the radar system field test. The approximated RCS ( $\sigma$ ) of 20000 m<sup>2</sup> of aluminum plate size of 1.5×1.0 m<sup>2</sup> is also calculated from the reference RCS value of 32 m<sup>2</sup> by measuring aluminum plate size of 0.3×0.2 m<sup>2</sup> [13].

Table 1.1. Comparison of range and minimum received power.

Range (m)	P <sub>r</sub> (nW)	P <sub>r</sub> (dBm)
40	3991	-23.989
60	788.8	-31.03
80	249.43	-36.03
100	102.17	-39.907
120	49.27	-43.074

140	26.59	-45.753
160	15.59	-48.072
180	9.73	-50.118
200	6.39	-51.948

### 3.2. Front-end Module Diagram

The X-band frequency front-end module diagram and its top view image of the actual implementation are shown Fig. 2 and Fig. 3. The evaluated system consists of a Sawtooth waveform generator, X-band frequency synthesizer, power amplifier, RF power splitter, mixer, low noise amplifier (LNA), antennas and handheld spectrum analyzer. The measured data from the spectrum analyzer is exported to calculate the distance of aluminum plate in MATLAB [14] software.

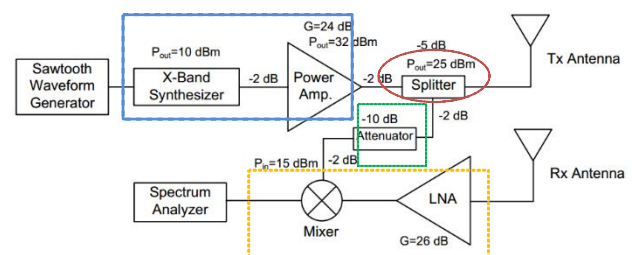


Fig. 2. Diagram of X-Band front-end module.

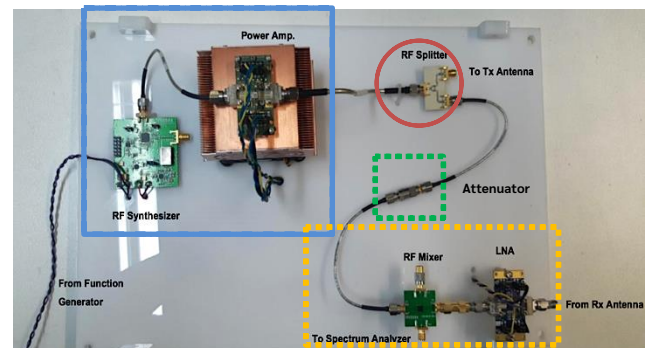


Fig. 3. X-Band front-end module for FMCW Radar.

### 3.3. X-Band RADAR Frontend Components

In this section, the components of X-Band Frontend module is presented. The function generator model GFG-8210A from GWINSTEK is shown in Fig. 4. It is used to generate the input sawtooth signal for the RADAR system in which it sweeps its output voltage between 4 volts and 9 volts with the frequency of 267 Hz as shown in Fig. 5. This generated waveform is fed to drive the X-Band Frequency Synthesizer in the second stage.



Fig. 4. Arbitrary Function Generator.

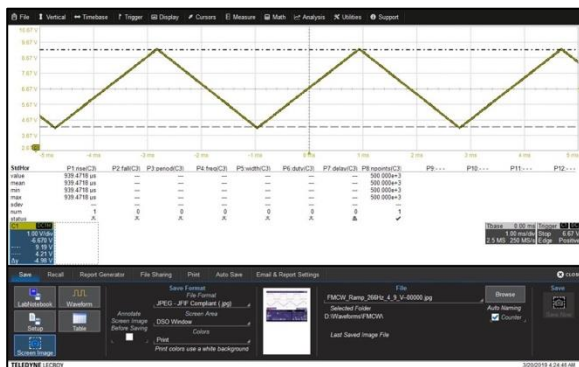


Fig. 5. Time Domain waveform of Sawtooth Signal at frequency of 267 Hz used to control X-Band Frequency Synthesizer



Fig. 6. X-Band Frequency Synthesizer.

Figure 6 shows the X-Band frequency Synthesizer based on Analog Devices' HMC769LP6CE [15], which internally consists of Voltage Controlled Oscillator (VCO) and fractional-N Phase Lock Loop (PLL) for generation of X-Band signal. The average output power level of this synthesizer is approximately 10 dBm as captured by the spectrum analyzer in Fig. 7.

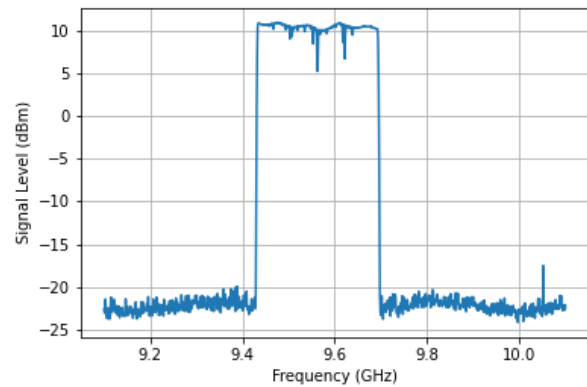


Fig. 7. Output power result of X-Band Frequency Synthesizer.

In the transmission part as shown in Fig. 2, a 24-dB gain X-Band power amplifier circuit with operating bandwidth of 6-12 GHz is used in the FMCW RADAR system. The amplifier circuit which is based on Qorvo's TGA2598-SM [16], which is a broadband driver amplifier, is shown in Fig. 8. Note that the circuit board is mounted on a copper heat sink. The output signal of the amplifier at the position of splitter output port before transmit antenna is captured by the spectrum analyzer with an average level of 22.8 dBm is shown in Fig. 9. This signal is then forwarded to the RF power splitter and then to the transmitted antenna.

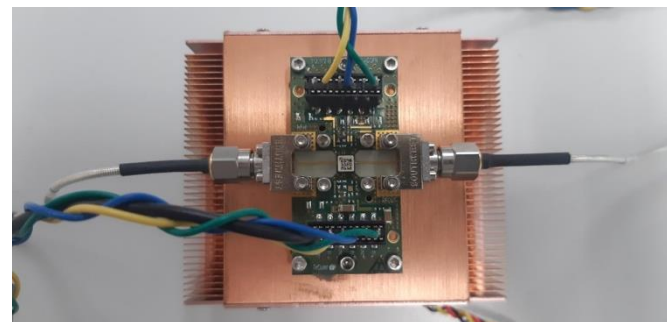


Fig. 8. TGA2598 X-Band Frequency Power Amplifier.

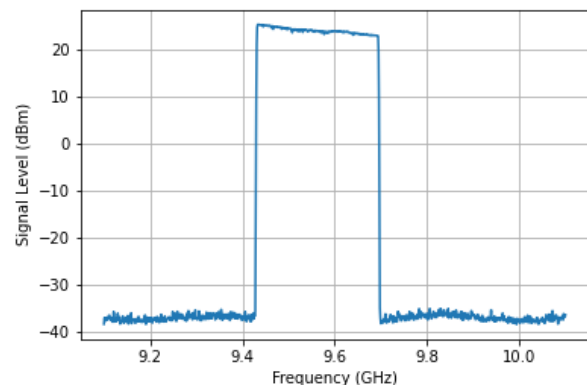


Fig. 9. Spectral power in frequency domain of X-band power amplifier circuit.



RF Power Splitter which is designed by the principle of Wilkinson Power Divider [17] on the RO4350B two-layer PCB [18] as shown in Fig. 10. The power splitter plays an important role in FMCW RADAR system as it divides the transmitted signal into two parts: one that is forwarded to antenna and another that is fed to the Local Oscillator (LO) port of an RF Mixer as the reference signal.

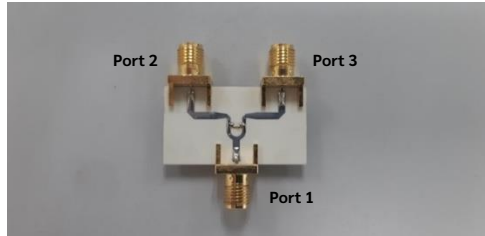


Fig. 10. RF Power Splitter.

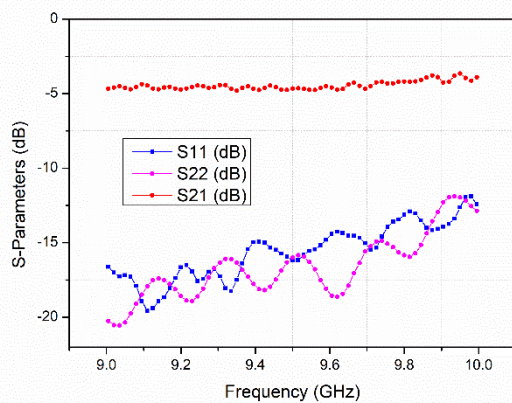


Fig. 11. RF Power Splitter S-parameters Measurement.

In the signal multiplication process between LO signal and received signal (reflected RADAR signal) of the RF mixer on the receiving part of the FMCW RADAR frontend in the diagram of Fig. 2, the intermediate frequency (IF) signal is used for the distance calculation of detected object. Note that the IF signal is the output of the RF mixer. This signal is then captured by the spectrum analyzer for the data analysis. Due to the loss of each cable approximated to -2 dB connected between circuits and forward transmission loss of RF power splitter of -5 dB as shown in Fig. 11. Figure 12 shows a measurement of the divided signal that came out from the RF splitter to LO port of the RF mixer. The average level of this signal is approximately 15 dBm.

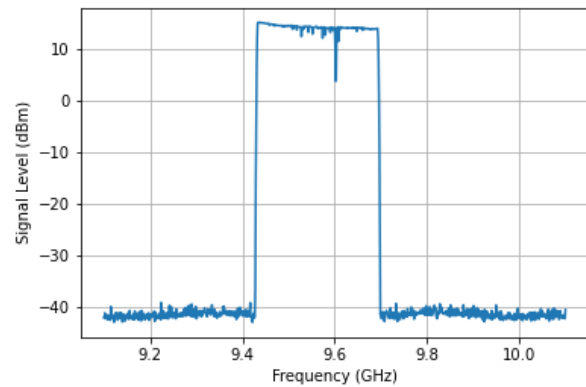


Fig. 12. Spectral power in frequency domain of transmitted signal from RF splitter to RF Mixer.

On the receiving side of the FMCW RADAR system, the reflected signal is detected by the receiving antenna and is amplified by a low noise amplifier (LNA) as depicted in Fig. 2 and 3. The low noise amplifier (LNA) has 25 dB small signal gain with lower than 2 dB noise figure. This LNA is based on Qorvo's 7-14 GHz QPA2609 evaluation circuit [19]. It is used to amplify the received X-Band signal. The LNA, as shown in Fig. 13, extends the operating distance of RADAR system by amplifying the reflected signal level from a distance object (aluminum plate in this case). The received signal of the FMCW RADAR system must be higher than the noise floor level or readable above the noise floor in the spectrum analyzer scale in order to analyze the performance of the frontend circuits.

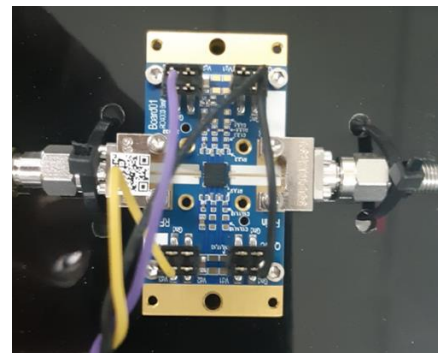


Fig. 13. X-Band Low Noise Power Amplifier.

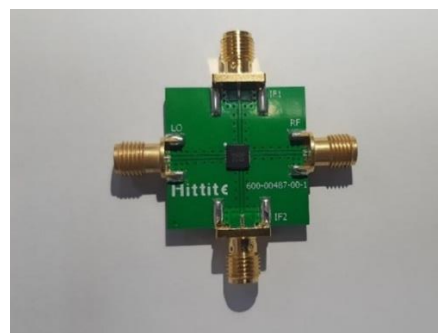


Fig. 14. RF signal I-Q mixer.

The power RF mixer model of HMC1056LP4BE, which is an GaAs MMIC I/Q mixer for 8-12GHz, from Analog Devices [20] is shown in Fig. 14. This type of I-Q mixer has an advantage over the conventional Heterodyne mixer. In Heterodyne mixer, the output mixed signal can be equaled to zero if the phase difference between real part and imaginary part of mixed signal is 90 degree. For the I-Q mixer, both real and imaginary parts of signal can be synthesized without this problem.

In order to detect the reflected signal that is lower than -90 dBm, the receiver must have high sensitivity. In this work, the FieldFox N9914A handheld spectrum analyzer is used for detecting the received signal. The PE9856/SF-20 Pasternack model pyramidal horn antenna with 20-dBi gain and 16.5 degree of beam width angle is used as the transmitted antenna [21]. The 3160-07 ETS-Lindgren model with 16-dBi gain and 26 degree of beam width angle is used as received antenna [22].



Fig. 15. Transmitted Antenna of PE9856/SF-20 Pasternack model (Blue) and Received Antenna of 3160-07 ETS-Lindgren (Red).

### 3.4. Field Test of Prototype

The field test of the proposed FMCW RADAR front-end module is verified at a pavement of an area within the National Science and Technology Development Agency (NSTDA) as shown in Fig. 15. and Fig. 16. An aluminum plate is used as object under test which can reflect the FMCW RADAR signal. There are three sizes of the aluminum plates used in our experiment: 0.3 m<sup>2</sup>, 0.8 m<sup>2</sup> and 1.5 m<sup>2</sup>. The distance was varied from 40 to 200 meters with an increment of 20 meters.



Fig. 16. Field test of X-Band front-end prototype.

## 4. Result Discussion

The spectrum analyzer displays the IF frequency response as shown in Fig. 17 when the object is at distance of 100 meters from the frontend system. By using the cliff top point search algorithm with measured data in MATLAB program, the detected IF-frequency is about 146.63 kHz. The max-hold function of spectrum analyzer is used to capture the result. From the result analysis, we observed that the position of the beat frequency is at the maximum level near the cliff of the graph. The positions of  $f_b$  at two other testing distances (120 and 140 meters) are also shown in the same pattern as shown in Fig. 18.

The resultant frequency domain curves from spectrum analyzer are exported into MATLAB in order to search for the position of  $f_b$  by optimization algorithm. Then, the optimized value of  $f_b$  is determined for each testing range.

Table 2. Comparison of range and beat frequencies from measurement and calculation.

Range (m) (Measure)	Range (m) (Calculate)	$f_b$ (kHz) (Measure)	$f_b$ (kHz) (Calculate)
40	42.26	57.44	60.83
60	59.59	86.16	85.57
80	81.79	114.88	117.45
100	102.087	143.60	146.63
120	121.91	172.32	175.065
140	145.85	201.04	209.45
160	168.03	229.76	241.3
180	180.22	258.48	258.79
200	207.19	287.20	297.54

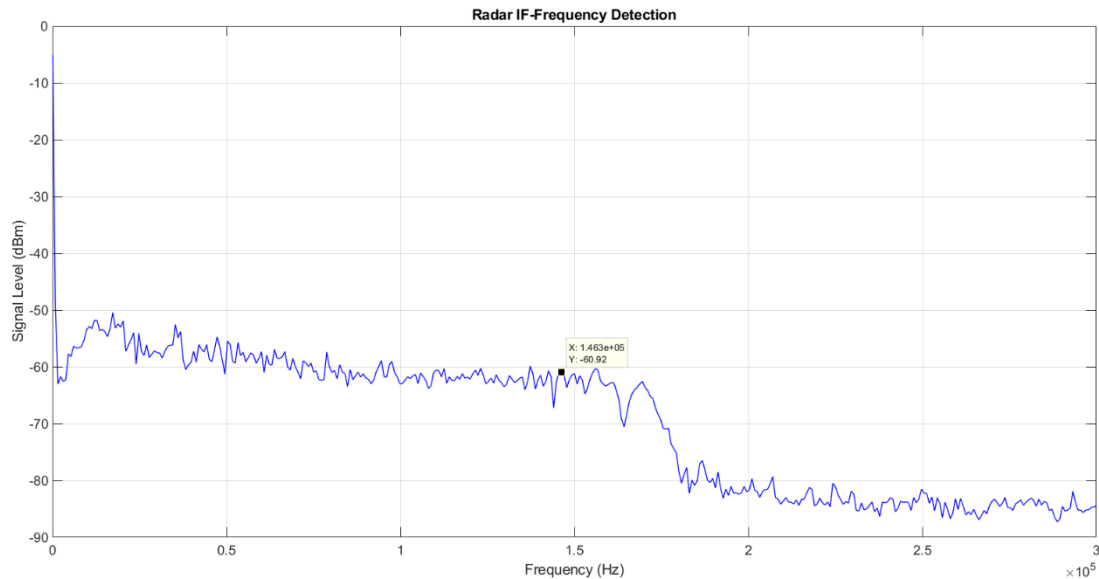


Fig. 17. Received IF-Frequency Signal for the testing object at distance of 100 meters.

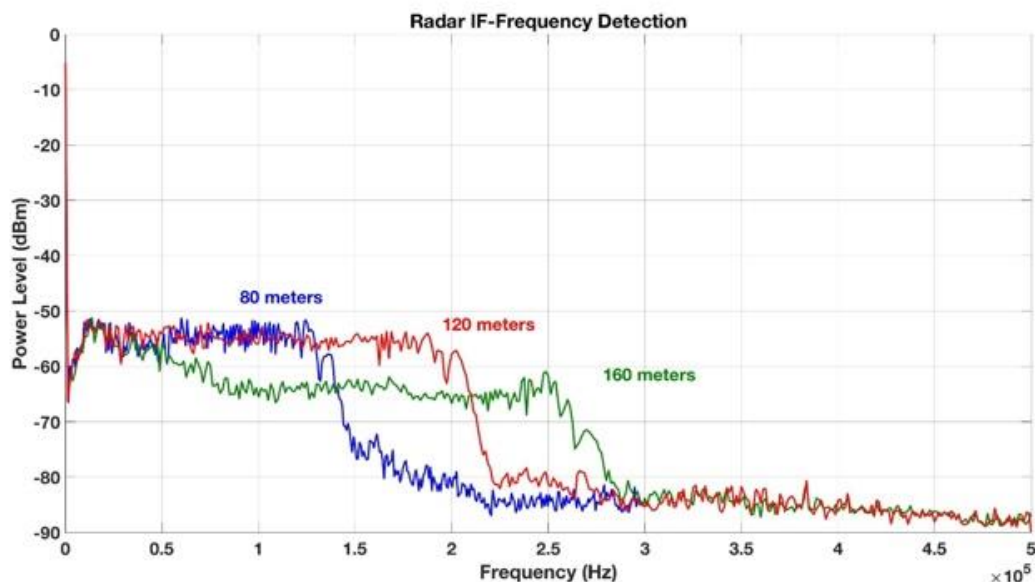


Fig. 18. Comparison of Received IF-Frequency Signal for the testing object at distance of 80 meters, 120 meters and 160 meters.

The calculated results of ranges and beat frequencies are summarized in Table 2. The maximum range of 200 meters can be achieved for our proposed FMCW RADAR system. The data of theoretical ranges and beat frequencies are compared with the calculated data. The actual range is measured by the measuring wheel tool. The theoretical beat frequency is determined by equation (2) with the physical parameters of the frontend system. The calculated ranges and beat frequencies are determined from the optimized value of  $f_b$  on each spectral curve in MATLAB. The optimized value of the beat frequencies can be determined with the error lower than 5.02 percent. The error comes from the delay and heating effect during the operation of each subsystem such as the active

transistor device in the power amplifier and LNA. From Table 2, the maximum error distance is about 13.25 meters at testing distance of 160 meters. When the testing distance is increased, the distance error did not change significantly which leads to the lower percentage error ratio.

Three different sizes of reflecting aluminum plates are used to measure the reflection capability based on the received power level measured by the spectrum analyzer. The received power level for each size of plate at different distance is shown in Table 3. We can notice that the largest size of the plate yielded the highest received power level. The received power is proportional to the radar cross section (RCS) area of the object. The average difference

value of received power for four distances between medium-to-small and large-to-medium plates are -5.26 dB (0.2979) and -3.8275 dB (0.4142), respectively. These values can be converted to power ratio per 1 m<sup>2</sup> unit of different area as 0.5957 and 0.5918, respectively. This is shown the consistency of relationship between the area of object under test and reflected signal level.

Table 3. Comparison of range and reflected signal strength in unit of dBm of different sizes of reflecting object.

Range (m) (Measure)	Small (0.3 m <sup>2</sup> )	Medium (0.8 m <sup>2</sup> )	Large (1.5 m <sup>2</sup> )
100	-69.5	-65.29	-60.31
120	-61.61	-58.83	-53.49
140	-72.37	-67.79	-62.31
160	-69.89	-66.16	-60.91

## 5. Conclusion

The X-Band FMCW RADAR frontend proposed in this paper can detect the object up to 200 meters of distance with lower than 5.02 percent error. The performance of the system can be further improved by increasing the receiving gain of the LNA circuits both for the X-Band and the IF-Band frequencies. Then the lower RCS object also can be detected at farther range. The field test of reflected power level ratio and plate size is presented. The difference values of ratio for each pair of object under test is lower than 0.66 percent.

## Acknowledgement

This project is supported by NECTEC Electronic Device and System (EDS) Platform Technology Research Fund.

## References

- [1] C. Jones and P. Pimdee "Innovative ideas: Thailand 4.0 and the fourth industrial revolution," *Asian International Journal of Social Sciences*, vol. 17, no. 1, pp. 4-35, Jan. 2017.
- [2] B. Yektakhah and K. Sarabandi, "All-directions through-the-wall imaging using omnidirectional bi-static FMCW transceivers: Imaging technique and performance evaluation," in *2018 IEEE International Symposium on Antennas and Propagation & USNC/URSI National Radio Science Meeting*, Boston, MA, 2018, pp. 1963-1964.
- [3] R. Kumar, J. Cousin, and B. Huyart, "2D indoor localization system using FMCW radars and DMTD technique," in *2014 International Radar Conference*, Lille, 2014, pp. 1-5.
- [4] Y. Shen, Z. Wang, L. Zhang, N. Hua, and X. Shen, "The design of internal calibrator in Ka-band FMCW space-borne SAR," in *China International SAR Symposium (CISS)*, Shanghai, 2018, pp. 1-3.
- [5] A. Mushtaq, W. Winkler, and D. Kissinger, "A 79-GHz scalable FMCW MIMO automotive radar transceiver architecture with injection-locked synchronization," in *2019 IEEE MTT-S International Microwave Symposium (IMS)*, Boston, MA, USA, 2019, pp. 690-693.
- [6] N. Teachapangam and M. Wongsaisuwan, "Sizing and positioning of cylindrical object based on the millimeter-wave radar system," *Eng. J.*, vol. 24, no. 4, pp. 171-181, Jul. 2020.
- [7] Y. Ju, Y. Jin, and J. Lee, "Design and implementation of a 24 GHz FMCW radar system for automotive applications," in *2014 International Radar Conference*, Lille, 2014, pp. 1-4.
- [8] J. Lin, Y. Li, W. Hsu, et al., "Design of an FMCW radar baseband signal processing system for automotive application," *SpringerPlus*, vol. 5, 2016, Art. no. 42.
- [9] A. Chaudhari, S. Prabhu, and R. Pinto, "Frequency estimator to improve short range accuracy in FMCW radar," in *2015 International Conference on Advances in Computing, Communications and Informatics (ICACCI)*, Kochi, 2015, pp. 640-644.
- [10] R. G. Strauch, "Theory and application of the FM-CW doppler radar," Ph.D. thesis, Department of Electrical Engineering, Graduate School of the University of Colorado, 1976.
- [11] "Frequency-Modulated Continuous-Wave Radar (FMCW Radar)." Available: <https://www.radartutorial.eu/02.basics> (accessed September 11, 2020).
- [12] S. H. M. Al Sadoon and B. H. Elias, "Radar theoretical study: Minimum detection range and maximum signal to noise ratio (SNR) equation by using MATLAB simulation program," *American Journal of Modern Physics*, vol. 2, no. 4, pp. 234-241, 2013, doi: 10.11648/j.ajmp.20130204.20.
- [13] M. Miacci, M. Rezende, and Z. Hag, "Basics on radar cross section reduction measurements of simple and complex targets using microwave absorbers," in *Applied Measurement Systems*. InTech, 2012.
- [14] MATLAB. (9.0.0.341360 (R2016a)). The MathWorks Inc.
- [15] Analog Device, "HMC769LP6CE Fractional-N PLL with Integrated VCO." Analog.com. Available: <https://www.analog.com/media/en/technical-documentation/data-sheets/hmc769.pdf> (accessed October 2, 2020).
- [16] Qorvo, "TGA2598-SM 6-12 GHz 2W GaN Driver Amplifier," Qorvo. [Online]. Available: <https://www.qorvo.com/products/d/da004199> (accessed October 2, 2020).
- [17] D. M. Pozar, *Microwave Engineering*. Hoboken, NJ: Wiley, 2012.
- [18] Rogers Corporation, "RO4000 Series High Frequency Circuit Materials," Roger Corp. [Online]. Available: <https://rogerscorp.com/>



/media/project/rogerscorp/documents/advanced-connectivity-solutions/english/data-sheets/ro4000-laminates-ro4003c-and-ro4350b---data-sheet.pdf (accessed October 5, 2020).

- [19] Qorvo, “QPA2609 7-14 GHz Low Noise Amplifier,” Qorvo. [Online]. Available: <https://www.qorvo.com/products/p/QPA2609> (accessed October 2, 2020).
- [20] Analog Device, “HMC1056LP4BE GaAs MMIC I/Q Mixer 8-12 GHz,” Analog Device. [Online]. Available: <https://www.analog.com/media/en/technical-documentation/data-sheets/hmc1056.pdf> (accessed October 5, 2020).
- [21] PASTERNAK, “WR-90 Waveguide Standard Gain Horn Antenna,” PASTERNAK. [Online]. Available: <http://www.pasternack.com/images/ProductPDF/PE9856-SF-20.pdf> (accessed September 11, 2020).
- [22] ETS LINDGREN, “3160 Pyramidal Standard Gain Antenna,” ETS LINDGREN. Available: <http://www.ets-lindgren.com/datasheet/antennas/pyramidal-standard-gain/4019/401901> (accessed September 11, 2020).



**Tiwat Pongthavornkamol** received his M.Sc. degree in Communication Engineering from The Sirindhorn International Thai-German Graduate School of Engineering, King Mongkut's University of Technology North Bangkok, Thailand, in 2012. He received his Ph.D. in Microelectronics and Solid State Electronics Engineering from Institute of Microelectronics, University of Chinese Academy of Sciences, Beijing, PR China in 2016. He is currently a researcher with the National Electronics and Computer Technology Center (NECTEC), Thailand. His research interests are RADAR System and RF-Microwave Circuit Design.



**Aman Worasutr** received the B.S. degree in Electronic and Telecommunication Engineering from King Mongkut's University of Technology Thonburi, Bangkok, Thailand, in 2018. He is currently studying M.S. degree in Information and Communication Technology for Embedded System Engineering at Kasetsart University. His research interests are Embedded System, Digital Signal Processing and RADAR System.



**Denchai Worasawate** received the B.S. degree from Kasetsart University, Bangkok, Thailand, in 1995 and the M.S. and Ph.D. degrees from Syracuse University, Syracuse, NY, in 2000 and 2002, respectively, all in electrical engineering. From 1998 to 2000, he was with Sonnet Software, Incorporated, Syracuse. During 2000–2001, he was with Anaren Microwave, Incorporated, Syracuse, where he designed a number of passive and active microwave devices. He is currently a Faculty Member of the Department of Electrical Engineering, Kasetsart University. His research interests include numerical electromagnetics, antennas, and microwave circuits and devices.



**La-or Kovavisaruch** received her bachelor's degree from King Mongkut's Institute of Technology Ladkrabang, Bangkok Thailand in 1993; M.Sc. degrees in Electrical Engineering from Imperial College, London, U.K., in 1995; M.Sc. degree in Electrical Engineering from the University of Southern California, USA, in 2001; and a Ph.D. degree in Electrical Engineering from the University of Missouri-Columbia, USA, in 2005. She is currently working as the laboratory head of the Location and Auto-ID Laboratory in the National Electronics and Computer Technology Center, Thailand. Her research interests are indoor localization, wireless communication, inventory, and warehouse management technologies.



**Kamol Kaemarungsi** received a bachelor degree in Electronics Engineering from King Mongkut's Institute of Technology Ladkrabang (KMITL), Thailand in 1994, an MSc. in the Interdisciplinary Telecommunications Program (ITP) from the University of Colorado at Boulder in 1999, and a Ph.D. in Information Science from the University of Pittsburgh in 2005. He was serving as the Thailand Chapter Chair of the IEEE Communications Society, Asia/Pacific Region 10 from 2012 to 2016. Formerly, he was the laboratory head of the Location and Automatic Identification (LAI) laboratory under the National Electronics and Computer Technology Center (NECTEC). He is currently the Research Director of Communications and Network Research Group (CNWRG) under NECTEC, Thailand. His research interests include ground penetrating radar, ultra-wideband sensors, wireless sensor networks, and indoor positioning systems.